energies

MDPI

Article

CSP Quasi-Dynamic Performance Model Development for All Project Life Cycle Stages and Considering Operation Modes. Validation Using One Year Data

Adrian Gonzalez Gonzalez [1], J. Valeriano Alvarez Cabal [2,*], Vicente Rodríguez Montequin [2], Joaquín Villanueva Balsera [2] and Rogelio Peón Menéndez [1]

[1] TSK, 33203 Gijón, Spain; adrian.gonzalez@grupotsk.com (A.G.G.); rogelio.peon@grupotsk.com (R.P.M.)
[2] Project Engineering Area, University of Oviedo, 33003 Oviedo, Spain; montequin@uniovi.es (V.R.M.); jmvillanueva@uniovi.es (J.V.B.)
* Correspondence: valer@uniovi.es

Abstract: The energy production of concentrated solar power (CSP) plants not only depends on their design, but also of the weather conditions and the way they are operated. A performance model (PM) of a CSP plant is an essential tool to determine production costs, to optimize design and also to supervise the operation of the plant. The challenge is developing a PM that is both easy enough to be useful during the earlier stages of the project, and also useful for supervision of plant operation. This requires one to be able to describe the step between the different modes of operation and to fit the response to transient meteorological phenomena, not so relevant in terms of aggregate values, but crucial for the supervision. The quasi-dynamic performance model (QD-PM) can predict the net energy exported to the grid, as well as all the key operational variables. The QD-PM was implemented using Matlab-Simulink of Mathwoks (MA, USA) with a modular structure. Each module is developed using specific software and a state machine is used to simulate the sequence between the operation modes. The validation of the PM is made using one complete year of commercial operation of a 50 MWe CSP plant situated in Spain. The comparison between the actual data and the results of the model shows an excellent fit, being especially noteworthy as follows the transients between the different CSP operation modes. Then, QD-PM provides an accuracy better than the usual PM, and, almost, as good as that of a fully dynamic model but with a shorter simulation time. But, the main advantage of the QD-PM is that it can be use not only in the feasibility and design stages, but it can be used to supervise the operation of the plant.

Keywords: CSP; performance model; simulation; transient modelling; plant data validation; power block; parabolic trough; quasi dynamic

Citation: Gonzalez Gonzalez, A.; Alvarez Cabal, J.V.; Rodríguez Montequin, V.; Villanueva Balsera, J.; Peón Menéndez, R. CSP Quasi-Dynamic Performance Model Development for all Project Life Cycle Stages and Considering Operation Modes. Validation Using One Year Data. *Energies* **2021**, *14*, 14. https://dx.doi.org/doi:10.3390/en14010014

Received: 9 November 2020
Accepted: 18 December 2020
Published: 22 December 2020

1. Introduction

Concentrated solar power (CSP) plants use solar radiation to produce superheated steam for electric power generation on a thermic cycle. There are CSP plants all over the world, totaling more than 5 GW [1] with really interesting growth rates.

CSP plants have two main blocks: the solar field (SF), and the power block (PB), that includes a thermal storage system (TES). The thermal energy absorbed by the solar field is used to produce steam at high temperature. The power cycle includes feedwater heaters, turbines, generators, condensers, and other elements of the Rankine cycle. The general schema of a CSP with TES is shown in Figure 1. This paper is focused on CSP plants with parabolic trough collectors that include thermal storage.

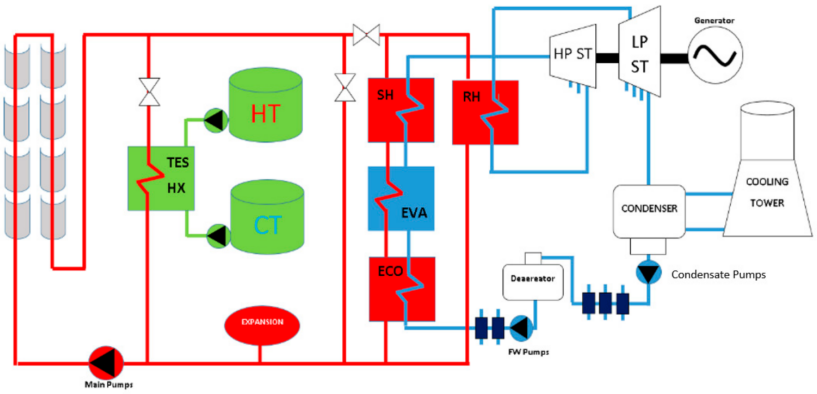

TES: Thermal Storage Tanks
HT: high temperature
CT: cool temperature
SH: Super heater
RH: Re heater

EVA: Evaporator
ECO: Economizer
HP ST: High Pressure Steam Turbine
LP ST: Low Pressure Steam Turbine

Figure 1. CSP Schema.

The levelized cost of energy (LCOE) of CSPs is being reduced in a constant way, but this reduction rate is lower than the one from PV. This improvement is not only achieved by reducing each systems' costs [2] but rather by improving plant performance. Due to political strategies, some countries are reducing their renewable energy bonus, as in [3]. Therefore, cost reduction acquires a dramatic relevance in order to allow CSP technologies to be able to compete in the pool with non-renewable energies and to expand to China, India and MENA region. As H2020 MUSTEC study [4] indicates, the cost and performance of CSP plants depend not only on single components (that can be manufactured in any country at a lower or higher cost), but mostly on the know-how of how to efficiently assemble and operate the entire station. Cost reduction came along with several changes in the business model. Clients no longer ask for an engineering procurement construction (EPC) approach but rather an EPC solution that includes operation and maintenance (O&M).

Since there is no current system for massive and economic electricity storage, energy must be generated at the time it is consumed. This issue is one of the main concerns regarding alternative power plant like PV or wind power. CSP plants could also include a thermal energy storage unit using hot molten salts, as they have good heat transfer rate and low drain capacity [5,6]. LCOE shows lower values when adding thermal storage, as stated on this review of implemented CSP plants [4].

In Section 2 of this article, a review of the state of the art on CSP plant performance models (PMs) is made, analyzing the developments done. Focusing on aspects such as the response to transients and other rapid meteorological phenomena. Given the relevance of the modes of operation, Section 3 will describe the layout of the plant and the main modes of operation. Section 4 refers to the development methodology of the QD-PM. It starts with the definition of the requested requirements to then define the general approach and describe in detail the elements that comprise it. Section 5 presents the verification carried out using data from a real plant in operation. Finally, it ends with the conclusions of the development carried out.

2. CSP Performance Models

The CSP plant electricity production depends on a combination of weather conditions, plant design and the way the plant is operated. Due to this dependence, in CSP projects it is essential to simulate plant operating conditions. The CSP performance model (PM) must simulate the amount of power and energy exported to the grid among other operational variables.

All CSP projects rely heavily on a proper development of the PM. It is implemented by the EPC contractor and will usually be part of the contract, so the PM outputs are bidded on. Before the inclusion of the PM into the EPC contract, the client and the independent engineer (IE) will review it.

The contractual performance model was used to calculate the energy generated by the plant. This would allow to evaluate the CSP Plant LCOE and to establish the economic feasibility of the plant. According to IRENA, in 2019, the average LCOE of CSP was 0.182 $/kWh. In the near future, it is expected that the LCOE drops down under 0.1 $/kWh. All this development is based on the TMY, which in most cases is an hourly basis file. This could be enough to evaluate the feasibility of the plant, but it would not be adequate for following up O&M activities on the plant. Despite that, depending on the site weather an hourly basis model could be enough. The hourly PM will impact harder on sites where there is rapid evolution vertical clouds, because the drop in solar radiation generate fast transients on the plant.

After the contract signature, the PM is also used to evaluate possible suppliers. It is possible to study if a certain increase in performance, or reduction in electrical consumption, is worth the extra cost. The PM is also an important asset in the design phase. All the design done during the project detailed engineering should be at least as good as what is stated in the PM. Otherwise, the performance guarantee will not be met.

When the commissioning stage ends, the performance test begins. The next phase is commercial operation; hence, the EPC team delivers the plant to the O&M team. Nonetheless, the plant is not yet fine-tuned, as O&M people could not have enough experience. Due to all these facts the PM output is extremely important, it will point out the weak points in terms of O&M and the path towards improvement. Table 1 does a sum up of how PM is involved in every project stage.

Table 1. Uses of PM in the CSP plant project stages.

Stages	Description
Proposal	It is used to define the main guarantees of the contract. The PM is given to the client as a description of the future plant performance. It is run using as input the average year meteorological data, allowing the client to compare the proposed design against the competitor's ones.
Decision-making	Compare the different parameters of different suppliers. A sensitivity analysis of the annual net energy will be used.
Design verification	Study the effect of mandatory design changes in the annual net energy guarantees.
Performance follow up	Use of the PM as guarantee evaluation tool. Discussion about penalties for non-compliance
O&M follow up	Supervision of plant operation and maintenance

There are plenty of CSP plant sub-system models for the main CSP blocks. Modelling the receiver optical performance according to collector's design, incidence angle, and heat losses, are generally well solved [7]. Based on that, the solar field models estimated the heat captured from irradiation into the HTF flow [8,9]. These physical models differ in how to use the meteorological data and how to include other parameters like maintenance factors, heat losses, etc. [10,11]. The power block uses a Rankine cycle, the same one as coal power. For this reason, it is common to develop the power cycle model using existing simulation software tools. Some authors try to improve the steady state model to include transients [12]. Further efforts were made using Wolfram's Mathematica 7 software in [13], although with a BOP is considerably simplified. In [14], a thermal cycle model using Modelica is developed and validated with data of SOLTERM, a CSP plant in Italy.

Since the 90s, complete CSP plant PM began to be developed. SOLERGY [15] and EASY [16] were developments of the Sandia National Laboratories, detecting the need to consider thermal losses (in the solar field, in pipes, ...). SEGS plant, located in the United States, made data used in many PM available for validation. The PM developed by Flagsol [17] was set up with a very high level of detail, so the model became very specific (as-built PM), although some elements such as the gas burners were not taken into account in the parasitics calculation. Also, the selected five min' time-step is a little excessive if we want to consider the effect of quick meteorological phenomena. It was validated with real data from SEGS and it entails that the annual error in gross data estimation is ±5%. Further development in this model was made, like including the thermal storage system [18]. In [19], Patnode developed a model of the solar field using TRNSYS simulation program (TRaNsient SYStem simultation Tool of Thermal Energy System Specialist, Wisconsin, USA) and using a simultaneous equation solving software (EES) to model the Rankine cycle. Parabolic Trough Thermodynamic Optimization (PATTO) can predict the performance of parabolic trough CSP plants under nominal conditions. The PATTO software [20] is limited to the evaluation at nominal conditions and they are also validated with SEGS data.

The System Advisor Model (SAM) [21] is a modelling software for renewable energy systems developed by the U.S. National Renewable Energy Laboratory (NREL). SAM combines annual time series of power production models with financial data to estimate the LCOE and other metrics for renewable energy projects. At first, SAM used the general-purpose commercial TRNSYS, a transient systems' modelling software package, described previously. NREL reformulated the CSP models into a new transient simulation framework written in C++, improving the simulation time [22]. It is currently the standard software for CSP technologies because it is freely distributed and has an adequate accuracy. SAM is used on the feasibility stage as an advisory model. However, the model has some limitations:

- Some variables and systems cannot be defined and there are restrictions on certain parameters. Not every CSP plant can be modelled, only the usual ones.
- Partial load is not accurately implemented.
- The capability of generating a standalone executable is limited. It could be done, since it is an open code, but it is not possible with the SAM user interface.
- Outputs are very limited and do not offer the variables needed for project life cycle.

SAM is widely used in academic papers [23,24] and, also, it is considered as a reference widely accepted in the feasibility study stage of the CSP plant projects. A relevant aspect in the PM development is the selection of the time-step. Maybodi et al. [25] use multi-year data sets with a range of different time step size (5, 15, 30 and 60 min) and different thermal storage capacities (4, 8 and 12 h) in a comparative study using SAM as a performance tool. This paper suggests that the use of a single year of hourly data gives a simplistic result. Using smaller time steps (e.g., 5 min) is likely to give a more realistic view of short-term operations that can be used for purposes such as optimizing control systems. On the other hand, longer time steps (e.g., 60 min) do not give a realistic representation at all. In addition, it is also indicated that when computational time is a concern, time steps of 15–30 min are likely to be enough to represent most operational situations.

Nevertheless, the meteorological conditions of different plant locations vary dramatically. In some cases, there are rapid evolution vertical clouds, which makes the operation of the solar field very difficult. An evaluation of the cloud transients was made by analysing a one-year dataset of direct normal irradiation (DNI) at Seville (Spain). It was concluded that the use of larger time steps entails greater loss of information, given that the average value of entrance and exit of the clouds is 3 min [26].

For net power prediction, it is of utmost importance to have the online parasitics model. A key figure in any electricity generation technology is the parasitics necessary to generate it. In [27], the parasitics of Andasol 3 plant, a 50 MWe Spanish plant, are evaluated.

3. Parabolic Trough CSP with Thermal Storage

3.1. CSP Diagram

The work presented in this paper is related to parabolic trough collectors CSP plant with TES, according to the schema of Figure 2. The collectors have a parabolic structure with the HCE placed in the focal length. There are different types of SF configurations: U shape and zigzag. Although the proposed PM allows configurations other than those, the CSP whose data is used for verification are made of U shape loops, which have four SCAs. Indeed, each SCA has 12 SCE and each SCE has four HCEs. The HTF flows inside the HCE until it reaches a temperature close to 400 °C (according to the specific physical characteristic of the heat transfer oils). BOP is the conjunction of all the system except from the SF, including solar steam generator, the Rankine cycle, the thermal storage system and the HTF heaters (designed to obtain the best economic result).

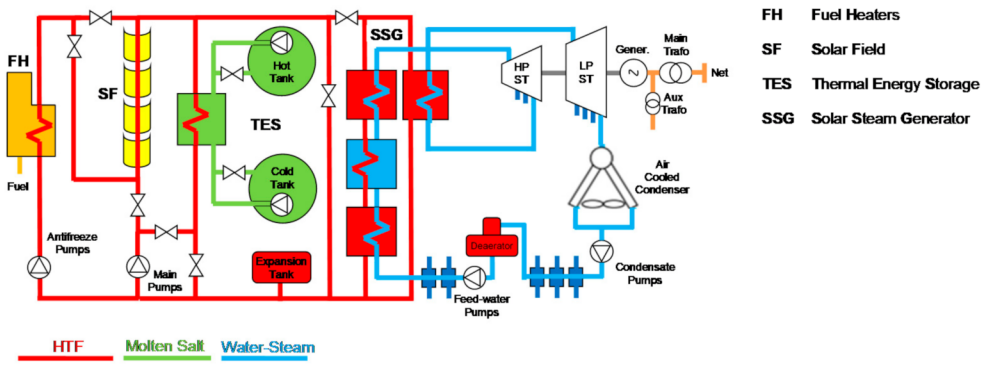

Figure 2. Generic parabolic trough layout.

3.2. Operation Modes

The most common operation modes are described here in a typical sequence of operational start up during sunny days. Before the CSP plant start up, the recirculation pump will start up to homogenize the temperature within the solar field. The next paragraphs detail the different operation modes. Figure 3 shows a detailed schema of every operation mode, where red lines indicate the flow passing through and the open valves are indicating in red.

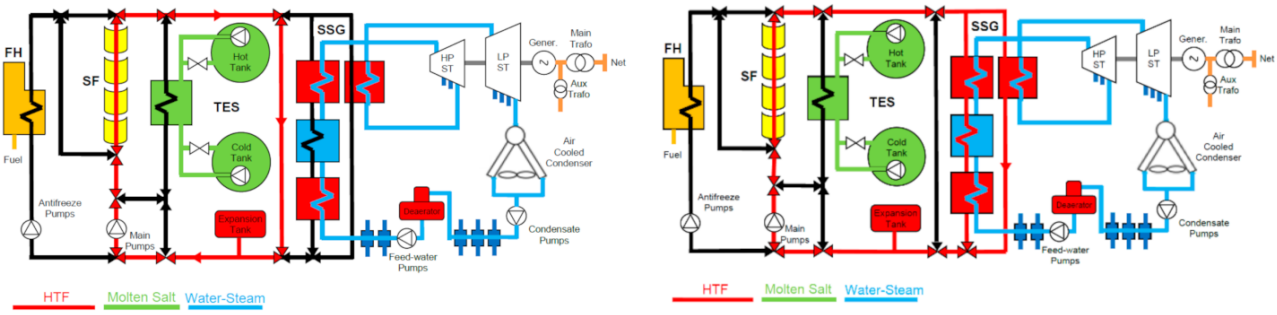

(**a**) Start up mode (**b**) SF→SG mode

Figure 3. *Cont.*

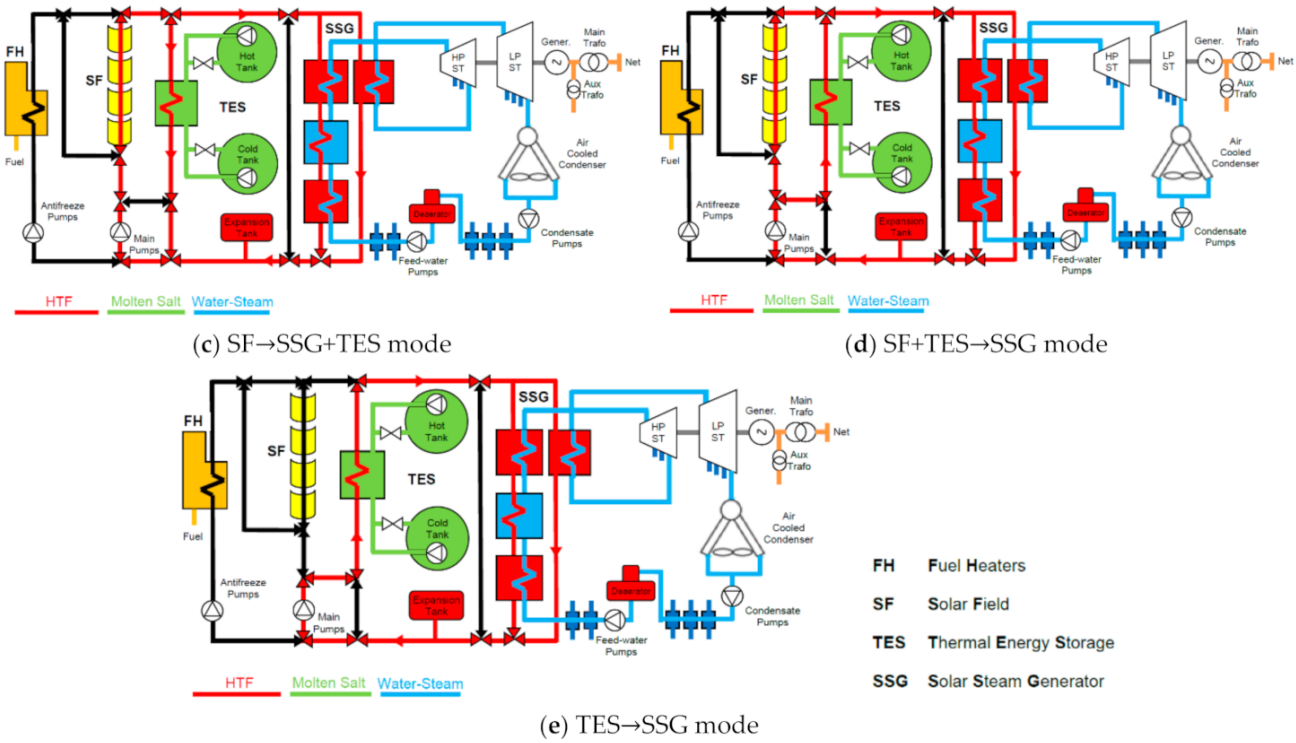

Figure 3. Generic parabolic trough operation modes.

(a) Start up Mode

At the start up, there is a similar temperature all along the SF. Short time after sunrise, the operator runs HTF main pumps at 30%, assuring the minimum flow needed through the HCE for focusing purposes. Once the SCAs are focused, the mass flow will be led through the bypass, until its temperature is adequate to go into the SSG or the TES.

(b) Solar Field to SSG Mode (SF->SSG)

In this operation mode, the production is directed from the SF to SSG. It is used when there is not enough energy in the SF to supply both the SSG and TES. This typically occurs after the start up.

(c) Solar Field to SSG and TES Mode (SF->SSG+TES)

If the SF produces enough energy, both SSG and TES are supplied. The transient between the mode SF->SSG and SF->SSG+TES will happen when there is enough radiation to give the minimum load to the TES and a complete SSG load.

(d) Solar Field and TES to SSG Mode (SF+TES->SSG)

The plant will shift to this mode when the energy from the SF is not enough to obtain nominal gross power, therefore a support of energy from the TES (when it is available) is required. This mode is reached usually after having operated in SF->SSG or SF->SSG+TES.

(e) TES to SSG Mode (TES->SSG)

When there is no solar radiation available, the energy stored in the Hot Tank will be used to generate electric power. HTF main pumps will direct the fluid through the oil-salt exchangers, heating the HTF. After passing through the SSG and releasing its energy, the fluid will return to the expansion system.

4. Quasi-Dynamic Performance Model

4.1. Performance Model Framework Requirements

The objective is to obtain a PM that can be used in every stage of the plant's life cycle with minor changes, and that fits well in all operation modes. The first step is to define the requirements by a board of CSP experts, with a lot of experience in CSP plant projects and operations. The main requirements are listed below in Table 2.

Table 2. PM Requirements

Concept	Requirements
Design & Flexibility	The model must allow the definition of non-usual systems, making it adaptable for different plant configurations and possible hybridization.
Accuracy	Maximum accuracy in net energy exported to the grid estimation (−3% in annual aggregate, not excess allowed). Good estimation of the process variables.
Outputs	Not only net power, but other key variables such as thermal power gathered by the solar field, thermal power charged in the TES, thermal power discharged, thermal power to SSG and off-line consumption.
Operation modes	All the operation modes in which the plant will operate need to be emulated.
Time step	At least 10 s, to consider quick transients.
Run time	As fast as possible, the PM will be also used in optimization stage. This is a very relevant requirement, as PM development time is several man-months.
Debugging & Learning Curve	The PM development schedule would be short enough to be useful in the proposal stage.
Standalone Black Box model	The model will be implemented and compiled at the feasibility stage, and it may be used by technicians without modeling experience

4.2. QD-PM Model Framework

The PM can be divided into two different parts: the wrapper code, which is the one managing the inputs/outputs, and the physical model that is the core of the PM. The PM algorithm structure schema is showed in Figure 4.

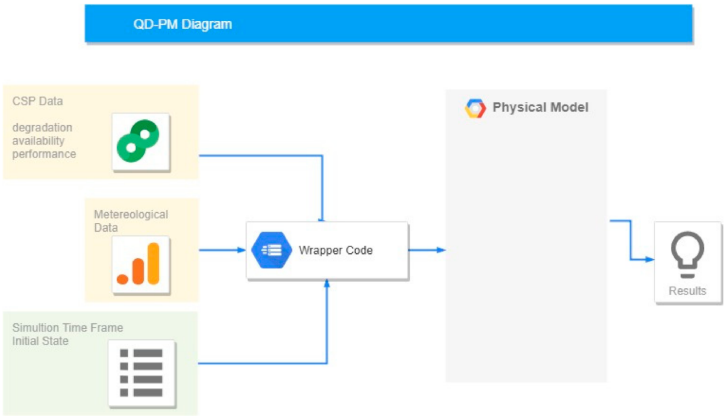

Figure 4. PM algorithm structure.

The main objective of the wrapper code is to read, filter and fix the inputs that will be used by the physical model. Afterwards, results are supplied to the physical model.

Regarding the physical model, it is implemented in Simulink with a Euler solver, and the time step will be 10 s. This would allow us to study very fast transients and phenomena throughout the CSP plant.

QD-PM integrates several models, as can be seen in the Figure 5, that will be described in detail in the next subjects.

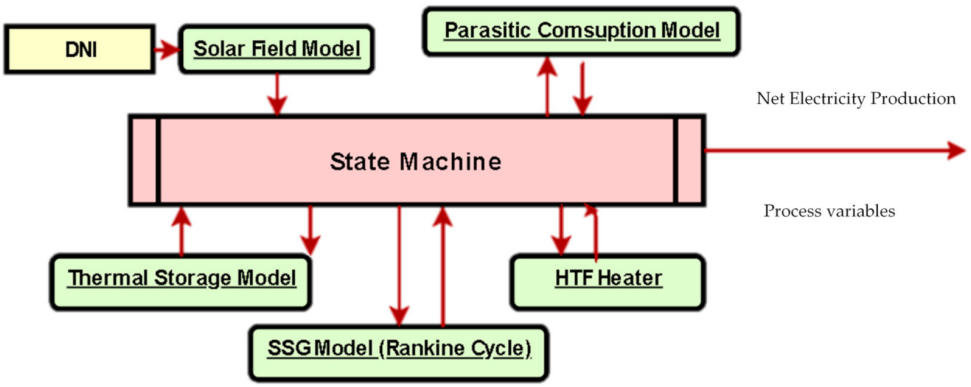

Figure 5. Physical Sub-Models.

QD-PM wrapper code was developed in Matlab-Simulink of Mathwoks (MA, USA). It was the chosen environment because it fulfilled all the necessary requirements: short developing periods, easy to debug, friendly human machine interface (HMI) and possibility to easily generate a standalone executable.

4.2.1. States Machine

All the control logic required for CSP operation must be implemented in the QD-PM. Defining the state machine in the PM is very complex, hard to implement and difficult to maintain. To avoid the excess of complexity, a new approach, called "QD-PM Energy manager", was developed. The algorithm considers the different systems as blocks. Those blocks could be in need of mass flow (demand) or they can provide mass flow (offer), as expressed in Figure 6. Then, the algorithm will match offer and demand thanks to a pre-established set of priorities. It will also consider the operative state of each system, the physical and design boundaries and the dynamic transients.

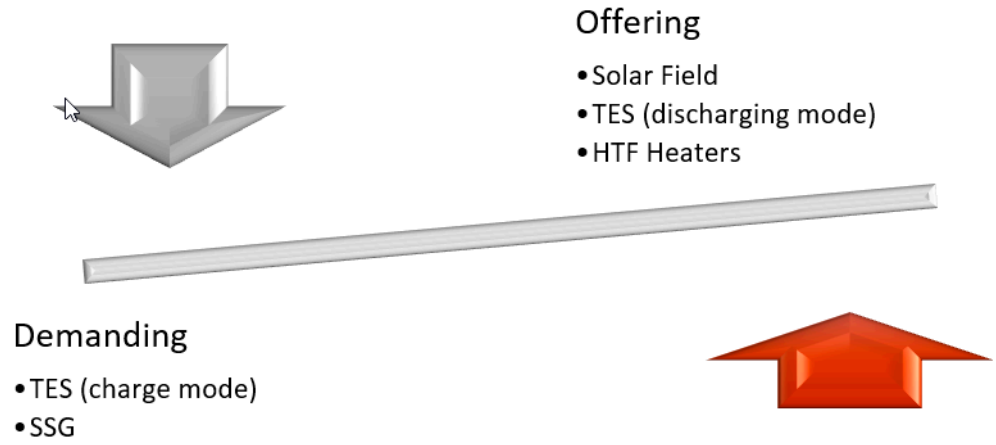

Figure 6. Energy manager system clustering.

4.2.2. Solar Field Model Description

The SF model calculates the elevation and azimuth at all times using a solar position algorithm (SPA) implemented by the NREL. The SPA has calculation uncertainties equal to ±0.0003° [28]. The calculation of the thermal power gathered by the SF was developed using the DLR standard [1]:

$$\dot{Q_{rec}} = G_{bn} A_{net} \cos(\theta_i) K(\theta_i) \cdot \eta_{opt,0} \cdot \eta_{clean} \eta_{endloss} \eta_{shad} - \dot{Q_{loss,rec}} \quad (1)$$

Equation (1) calculates the amount of thermal power that reaches the HTF. In this equation, G_{bn} is the DNI, A_{net} is the mirror area available (it is 500,000 m^2 in the validation). $\cos(\theta_i)$ is the incident angle cosine. $K(\theta_i)$ is the incident angle modifier, which is the factor that fits the performance of the collector for non-perpendicular sun beams. $\eta_{opt,0}$ is the receiver optical efficiency. η_{clean}, is the cleanliness factor for both mirrors and tubes (measured with a reflectometer). $\eta_{endlosses}$ is the coefficient that represents the energy loss due to the length of the SCAs. η_{shad} is the factor than models shading from one collector to another because of the lower sun elevation angle and finally, $\dot{Q_{loss,rec}}$ are thermal losses in the HCE:

$$\eta_{endlosses} = 1 - df \frac{\tan(\theta_i)}{l_{SCA}} \quad (2)$$

where l_{SCA} is the length of the SCA (it is 70 m in the validation), df is the focal length (it is 1.7 m in the validation) and θ_i is the incident angle:

$$\eta_{shad} = \frac{|\sin(e)|\, df}{|\cos(a)|} \quad (3)$$

where e is Sun elevation, a is Sun azimuth and df is the focal length (it is 1.7 m in the validation).

First, there are certain losses in the HCE; they are calculated based on the experiments made by the NREL [29]:

$$\dot{Q_{loss,rec}} = \left[A_0 + A_1 \left(T_{HTF} - T_{amb}\right) + A_2 \, T_{HTF}^2 + A_3 \, T_{HTF}^3\right] n_{loops} \, l_{loops} \quad (4)$$

where n_{loops} is the number of loops, l_{loops} is the length of the loop (it is considered 600 m in the validation), T_{HTF} is the bulk temperature of the HTF inside the HCE, T_{amb} is the average ambient temperature measured in the meteorological station.

Every coefficient of the equation above is detailed in Table 3 below.

Table 3. Coefficients used for losses calculation.

Factor	Value
A_0	4.05
A_1	0.247
A_2	−0.00146
A_3	5.65×10^{-6}

Until now, the output of the model is the thermal power. Although the model is quite simple, it is enough to give a great accuracy. However, the SF has a great thermal inertia. To include this feature in the model, the model considered that the SF was divided into blocks, each of them having mass and energy conservation equations. This allows transforming the SF model from static to dynamic.

A typical CSP plant of 50 MWe rated power usually has from 20 to 30 min of thermal inertia at a steady state. It will depend directly on the amount of the HTF in the solar

field which is given directly from the number of loops and the layout. This physical phenomenon needs to be assets correctly because is the one responsible of:

- Extending the power generation after the sunset, due to the energy stored in the HTF volume located in the solar field.
- Mitigating the impact of the clouds in the power generation.
- Starting every day the operation. If this impact is not considered the QD-PM would start much faster than the plant does.

To include this feature in the model, the model considered that the SF was divided into blocks, each of them having mass and energy conservation equations. This allows transforming the SF model from static to dynamic.

In a dynamic model, the output will be the amount of mass flow and temperature of the HTF in the outlet of the hot header. On the other hand, temperature will be calculated using energy conservation equations:

$$\int dh = \frac{1}{M} \int (\dot{m_{inlet}}\, h_{inlet} - \dot{m_{oulet}} h_{outlet} + \dot{Q}_{ABS}^{MAX})\, dt \tag{5}$$

$$T_{HTF} = f(h_{HTF}) \tag{6}$$

where $\dot{m_{inlet}}$ is the inlet mass flow, h_{inlet} inlet mass flow specific enthalpy. $\dot{m_{oulet}} = \dot{m_{inlet}}$ since the PM works with mass flow and it will not vary all along the SF, and M is the mass in the solar field. The nominal SF outlet temperature would be 393 °C. Thermal losses considered from the SF outlet to the BOP inlet are typically next to 2 °C, and the nominal solar field inlet temperature considered in the model is 293 °C.

Finally, there are operational restrictions that need to be emulated by the QD-PM, e.g., the flow through the HCE must be greater than the minimum required for turbulent regime (usually around 2 kg/s).

4.2.3. TES Model Description

The TES is composed by a pair of tanks, one hot and one cold, with 8 salt electrical heaters (antifreeze purposes) in each tank, a set of HXs (Heat Exchangers) and pumps for cold and hot salt.

The TES modelling is, also, dynamic, and it is based on the following equations:

$$\int dM = \int \left(\dot{m_{inlet}} - \dot{m_{oulet}}\right) dt \tag{7}$$

$$\int dh = \int \left(\frac{\dot{m_{inlet}}\, h_{inlet} - \dot{m_{oulet}} h_{outlet} + M_0\, h_0 + \dot{Q}}{M} \right) dt \tag{8}$$

$$T_{salt} = f(h_{salt}) \tag{9}$$

where $\dot{Q}$ is the thermal power introduced in the salt mass by the electrical salt heaters, M is the total mass in each of the tanks, $\dot{m_{inlet}}$ is the salt mass flow entering each tank, h_{inlet} salt inlet mass flow specific enthalpy, $\dot{m_{oulet}}$ is the salt mass flow leaving each tank, h_{inlet} salt outlet mass flow specific enthalpy. The Salt/HTF HX is modelled using $\varepsilon - NTU$ method [30].

4.2.4. SSG & Rankine Cycle Model Description

The power cycle model is divided into a SSG model implemented in Simulink (to model heat transfer and thermal inertia) and a Rankine cycle model implemented in the specific software Thermoflex.

The steam generation system consists of four heat exchangers: superheater, boiler, economizer and, usually, the reheater. The HTF enters the HX to produce superheated steam. This happens after quite some time, as there is an important amount of water in the boiler, which takes time to heat up. As already stated, HXs are simulated in the QD-PM

using the heat exchanger effectiveness ($\varepsilon - NTU$) method. The HX performance in this QD-PM would be 95%. All the exchangers have a static model for them, except from the boiler, simulated considering its thermal inertia and the transient phenomena (like in the startups). Operators must consider not to exceed the admissible ramp and the thermal shock in the HX. The output steam obtained from the SSG is superheated, and it will be led to the ST inlet to generate electricity. This SSG model is made using MATLAB-SIMULINK R2013b. Figure 7 shows a typical 50 MWe Rankine Cycle layout with five steam turbine extractions and the deaerator.

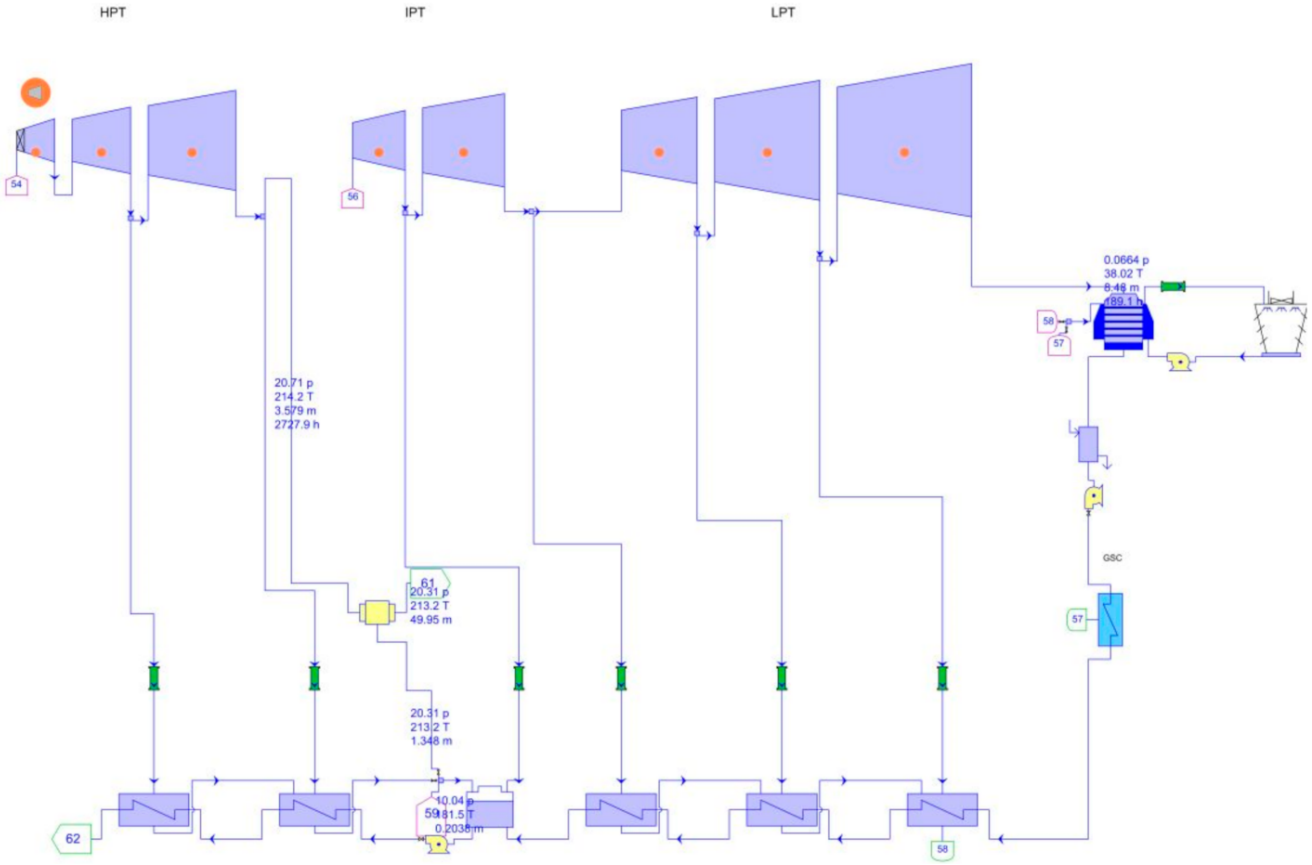

Figure 7. Thermoflex diagram for a 50 MWe Rankine Cycle.

The superheated steam is introduced in a Rankine cycle, as showed in Figure 7. It is modelled using Thermoflex commercial software. Thermoflex is a well-known, widely validated thermodynamic software for power cycle simulation. The inputs of the model are: Wet/Dry bulb temperature, steam temperature and steam mass flow. Thermoflex outputs are enthalpy, pressure, temperature, and mass flow of each point of the thermodynamic cycle.

However, the steam turbine has physical boundaries like maximum increasing inlet rates, among many others. These conditions are usually defined by suppliers. For this reason, the static model is not good enough. Then, in order to obtain a quasi-dynamic model, a multiple static snapshot was made, with enough cases (combination of the Thermoflex inputs) to model the Rankine cycle correctly. As the models generated in Thermoflex are static, it is necessary to introduce the limitation that eventually generates the transients. For the purpose of dynamical modelling the plant's behavior, a control strategy was developed, as Figure 8 shows.

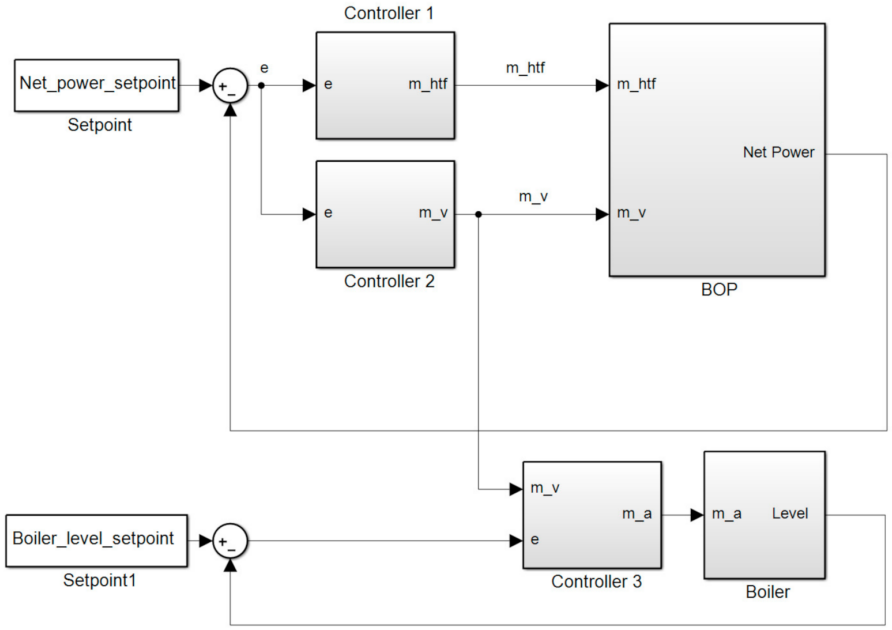

Figure 8. Sketch of the BOP control system.

The QD-PM control system emulates the work of CSP plant human operators. The electric grid defines the Net_power_sp, e.g., 50 MWe in a typical CSP plant in Spain (due to the state regulation), and the Boiler_level_sp is fixed depending on the operation mode (if it is starting up or at nominal state). The boiler level controller, Controller 3 in Figure 8, is a feedforward that considers the actual level of the boiler, the amount of steam mass flow leaving the boiler and the amount of feedwater mass flow entering the boiler. The net power controllers, Controller 1 and Controller 2 in Figure 8, are PID controllers affecting the same system.

The water/steam cycle is a very complex system. The static model provided by Thermoflex does not take into account the high pressure turbine (HPT) nor low pressure turbine (LPT) bypass. Those elements are controlled by their start up curves, which clearly define if the steam has enough quality to enter the turbine. Otherwise, it is bypassed and led to the condenser or to the ACC. The quasi-dynamic PM is generated from the set basis of static models generated with Thermoflex, and according to the control strategy.

Figure 9 shows the solar resource of a typical summer day, by means of the DNI and the ANI. The ANI is defined as $ANI = DNI * \cos(\theta_i)$ where θ_i is the incident angle. The yellow line represents the gross efficiency during the SF-> SGS and SF->SGS+TES modes of the plant, the line above this one is the QD-PM estimation, which is almost perfect. This was possible due to the modeling strategy, the QD-PM uses Thermoflex to calculate Rankine cycle efficiency. It is also remarkable how the QD-PM is capable of predict the behavior of the efficiency during the star-up process, we can affirm that this transient is well represented. Finally, the red line represents de gross efficiency during the TES->SGS mode, which is a little lower given the fact that the steam turbine works at a lower load with a lower steam temperature.

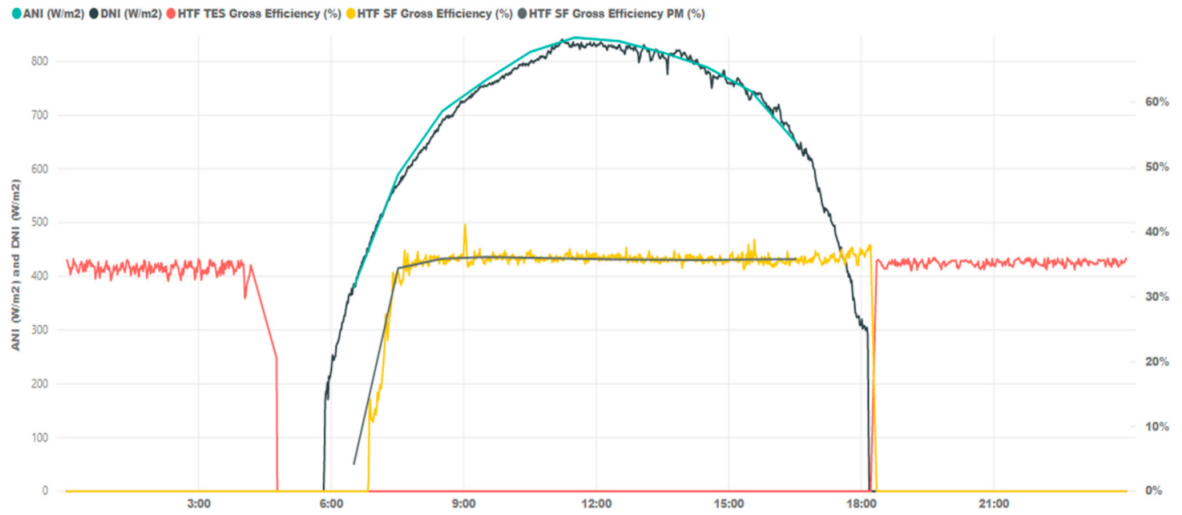

Figure 9. Turbine efficiency vs DNI.

4.2.5. Online/Offline Parasitics

In the QD-PM, all the main online parasitic consumptions are calculated using a fluid dynamic engineering simulation software, called AFT Fathom. This software calculates the hydraulic power of the pumps using the real or estimated layout, the current operation mode and the supplier data. As Fathom´s output is the hydraulic power, it is necessary to add the mechanical and electrical performance based on the pumps' datasheet. This calculation is made for: HTF main pumps, heater pumps, recirculation pumps, feedwater pumps, condensate pumps... Other auxiliary consumption that becomes offline parasitics when the plant is in shutdown is calculated using the supplier´s data such as the heat ventilation air conditioning (HVAC) system, CCTV, water treatment plant (WTP), lights, etc, including the data in the QD-PM.

Figure 10 shows an example of the effort done to calculate the hydraulic power of the HTF main pumps.

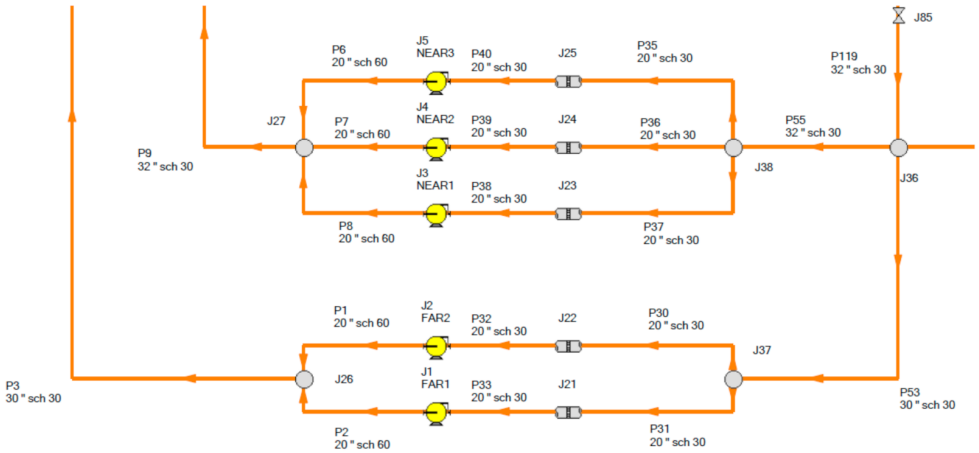

Figure 10. Fathom diagram (detail).

5. Validation

QD-PM simulates the real operation of a CSP plant using meteorological data as an input. It also calculates the energy output and other intermediate variables. The model will only be useful if the values obtained are very close to the real ones. Many verifications of every QD-PM sub-model was made using real data from commercial operated CSP plant. On basis of those results, QD-PM was adapted, introducing more complexity in sub-models to give the necessary accuracy.

Validation uses a whole year data set of the main variables captured from a 50 MW CSP plant located in southern Spain. A massive data extraction was done from the CSP plant data log, throughout the KKS of each instrument. This dataset should be analyzed in order to detect errors or outliers. The whole year dataset is composed of 15,768,000 rows for each variable (one each 2 s), with a very low percentage of missing values and outliers. This amount of data is enough to test the accuracy of QD-PM in every operational mode. A comparison between real data and QD-PM result is done to check their capability to do continuous net energy forecasting.

One of the QD-PM requirements is the capacity to follow up the daily prediction capability. It is complicated to achieve a great accuracy in this scenario due to the following facts:

- Human factors, as these plants still have medium level of automation and operators have learning curves.
- Variations between the designed operation and the one carried out by the O&M team, based on simplifications or improvements.
- Non-usual operation, which directly affects the performance, e. g. variation on the strategy due to the premium time schema.

5.1. QD-PM vs. Real Data Aggregate

QD-PM must be defined and compiled in the feasibility stage as a black box model. Taking this into account, certain variability in the results of the validation process can be expected, as there may be some changes in the construction stage.

Figure 11 shows the accuracy of the model in daily basis. Every dot represents one day of the year. The position of the dot in the vertical axis reflect the relative error (MRE) calculated as daily net energy against QD-PM estimation. As QD-PM calculate the power generated in MW, we calculate the power estimation root mean square error (RMSE) against real value. The horizontal axis reflects the RMSE value. Most of the days, both error measures are very low. But it can be seen than in some days (dots in the far right of the graph) where there are very good values of MRE, but with big error in power estimations (RMSE). These days are typically either winter days or days when the O&M strategy is very different to the one implemented in the PM. It is usual that in winter days the production profile is very different, but the aggregate is really close.

Many days, relative MRE values are around 0% of relative error. Most days (316 days, 86.6%), the relative MRE is between $\pm 5\%$, a value that is considered good enough for plant supervision. There are some cases with greater RMSE, which were reviewed. Those days correspond to the ones with abnormal operation strategies or bad weather conditions, where the expertise (or the mistakes) of the human factor were the determining factor. The result is very good when plants' operator follows the strategy programmed in the QD-PM, but if it is different, the PM, naturally, is not so precise. An example is the morning start up, which is very difficult to simulate accurately because it depends on the weather, the plant status and, above all, the practice the operator has in making all decisions during the start-up process.

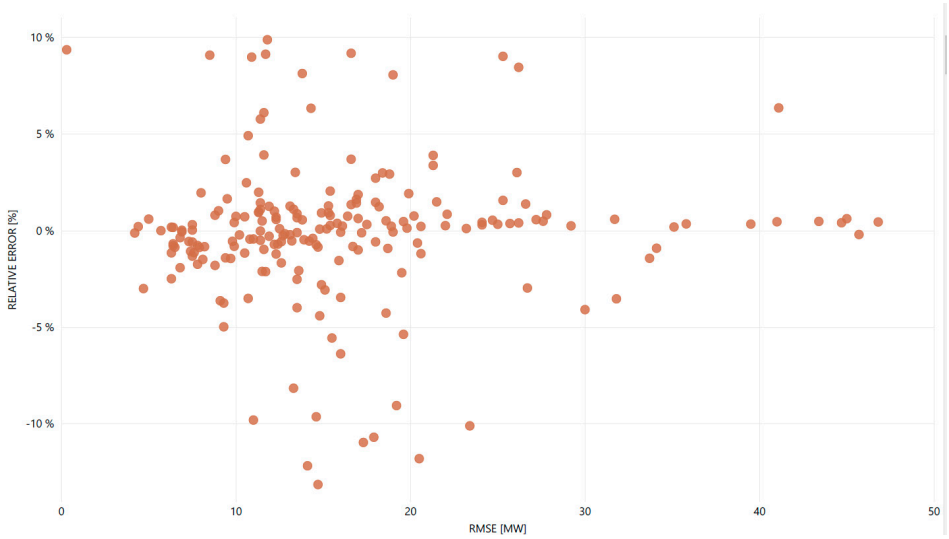

Figure 11. Daily aggregate net energy MRE vs. RMSE.

On the other hand, the same study was done in a month basis. The accuracy in the aggregate values is very important, because the guarantees of CSP plants' EPC contract are based on them. As can be seen in Figure 12, every month except from one, the monthly aggregate has a relative MRE lower than ±5%. It also exposes that 50% of the months stay between ±3% of relative error.

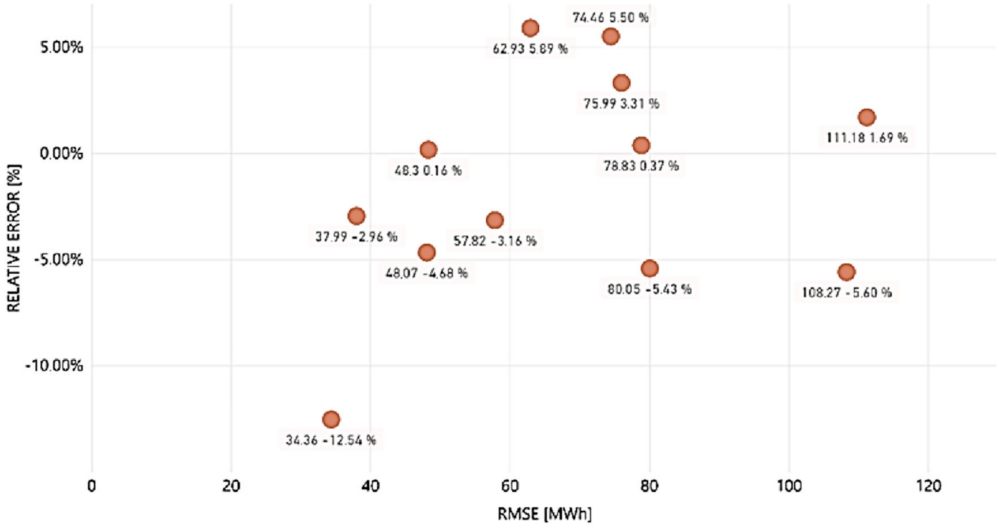

Figure 12. RMSE of monthly aggregate net energy.

For the whole year, the aggregate value estimated by QD-PM is 97.88% of the real one. The QD-PM shows on aggregate data a lower undershoot error, validating that PM is very adequate to establish CSP project guarantees.

For the purpose of fully fulfill the goals, it was convenient compare the accuracy with the performance model most widely known: SAM For do this, a SAM model is developed using the plant data and run against the same validation data set. The most important variable, the one that is contractually binding is the net power. Any shortfall on this regard would entail liquidation damages (LD). In the Table 4, there are two coefficients of determination of how good both the QD-PM and the SAM fits the energy gathered by the solar field in the plant. It is clearly stated that each model fits very well the real data, but the PM is slightly better.

Table 4. R^2 Net energy daily aggregate validation comparison between QD-PM and SAM.

Daily Aggregate Net Power	
QD-PM	SAM
0.958	0.893

Daily comparison is a very complex validation, it depends on to many variables among which there are those impossible to predict with precision, e.g., the meteorological forecast which could lead different operation strategies. Other important variable would be the operator, how aggressive or conservative operating the plant. QD-PM performance is clearly better when the meteorological conditions are changing.

In the end, the deviation generated by those differences would be compensated during the month and during the year, i.e., why the monthly coefficients of determination are higher than the daily. Table 5 shows the first monthly validation comparison in which the R^2 are higher than before, in this case the PM fits almost perfectly the plant data.

Table 5. R^2 Net energy monthly validation comparison between PM and SAM.

Monthly Aggregate Net Power	
QD-PM	SAM
0.997	0.972

5.2. QD-PM vs. Real Data Continuous Daily Comparison

The QD-PM must consider factors like weather conditions, grid availability, scheduled or unscheduled maintenance, and human factors. In order to be useful in all project stages, as it is required, QD-PM must fit the continuous real data, not only average values. To validate if all these issues are solved by QD-PM, a comparison between real data and model results was made. It is normal to display the data in day by day graphs, for supervision. In all figures, dashed lines are used for QD-PM results and the continuous ones are used for real values measured in plant.

Figure 13 shows the evolution in a sunny summer day (13 August) as an example of the most usual sequence of operation modes. The bars below the graph shows the operation mode in which the plant is. The accuracy of the estimation of the net energy generated (red line) is very tight, with a very slight delay in the mode of operation changes. All values are measured in MW (thermal for SSG values and electric for Net energy ones). The net energy generated is the area under the curve.

Vertical dashed black lines indicate the change between the different operation modes. The band situated under the graph details which is the operation mode. The evolution of the estimation of the thermal energy of the SSG (dashed red line) shows the effect of the inertia of both piping and equipment. The monitoring of the energy generated (blue line) is very tight, with a very slight delay in the changes in the mode of operation. It is extremely precise in stationary performance, and lower at the evening because there is an energy support from the TES system, whose operation mode and the amount of salt is slightly different from the one defined in the design phase. The output of the QD-PM when the plant starts up clearly describes the transition between the different operation stages, besides, it matches very precisely the real values.

Unfortunately, not every day of the year is a sunny summer day with enough sun insolation to follow this nominal operation. The discrepancies with the model are greater when the operating conditions are changeable, or the irradiation is either low or fluctuating due to cloud transients. To show how QD-PM output fits real one, a random day of the months of every season in shown in the Figure 14. To select what day of the month to show (26th), the only restriction placed was that the operation needed to be affected by quick changing weather conditions, at least once time. Four graphs are included: the SF thermal

power (orange lines), thermal energy stored in the TES system (red lines), SSG thermal power (brown lines) and net energy (green lines). The first two are the thermal energy sources, the third one is the thermal energy as an input in the thermal cycle and the last one is the net energy produced.

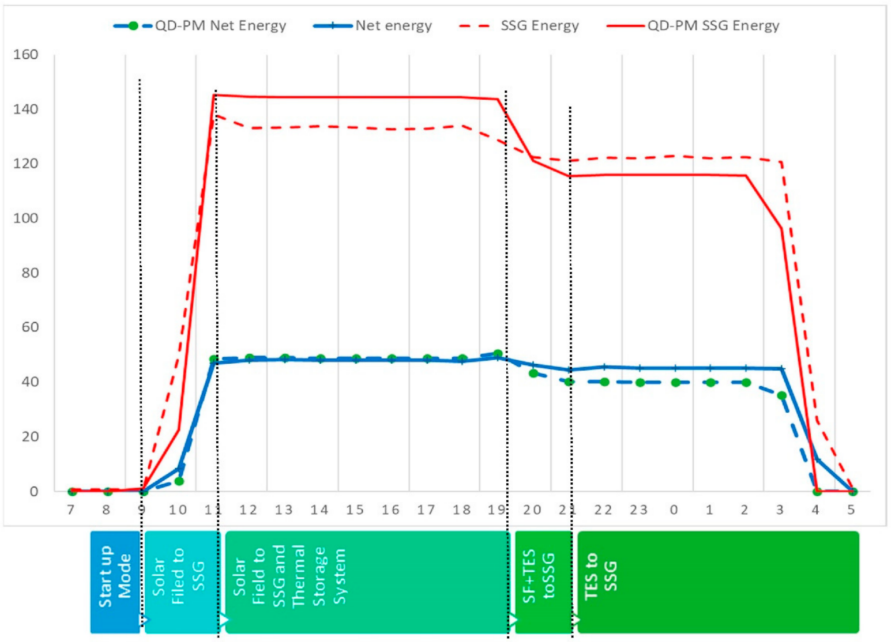

Figure 13. Operation mode evolution for a typical summer day (hourly data) [MW].

In April (Spring), for example, there are many clouds all day long. The QD-PM reacts more aggressively to the clouds than the real plant due to the reduced thermal inertia. This fact is shown in all figures but in the stored energy one. On that one, QD-PM predictions perfectly fit reality. The overreaction of QD-PM was expected, and it is partly explained due to the changes introduced during plant construction.

In August (Summer), the example day is sunny and stable, so real plant data and estimations are almost a perfect match. It is also an easy-to-operate day, as the plant is already hot due to a long operation day the day before. All plant conditions are considered as nominal.

In October (Fall), all four models predict accurately in such a difficult day, there are periods with sun and periods without it. As in spring days, the key parameter here is higher plant thermal inertia. It is important to note that in this kind of days the human factor is really important.

In December (Winter), it is important to consider that the example day is the 26th and the cosine effect, in the energy gathered by the solar field, is maximum. That entails, together with the fact that it is a cloudy day, a difficult plant operation. Nonetheless, the solar field model fits quite well. Those factors previously stated are the reason why the energy stored is very different, even though the energy available to charge this day is negligible.

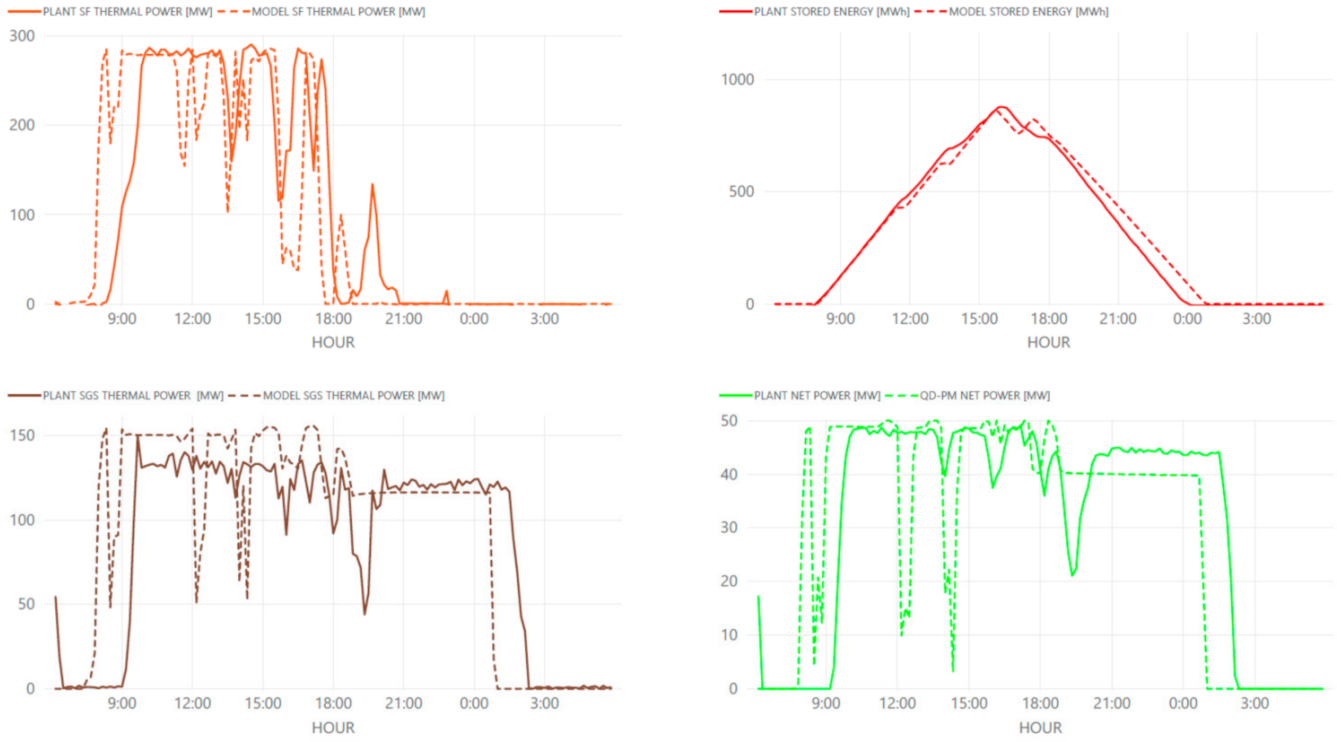

(**a**) 26th of April

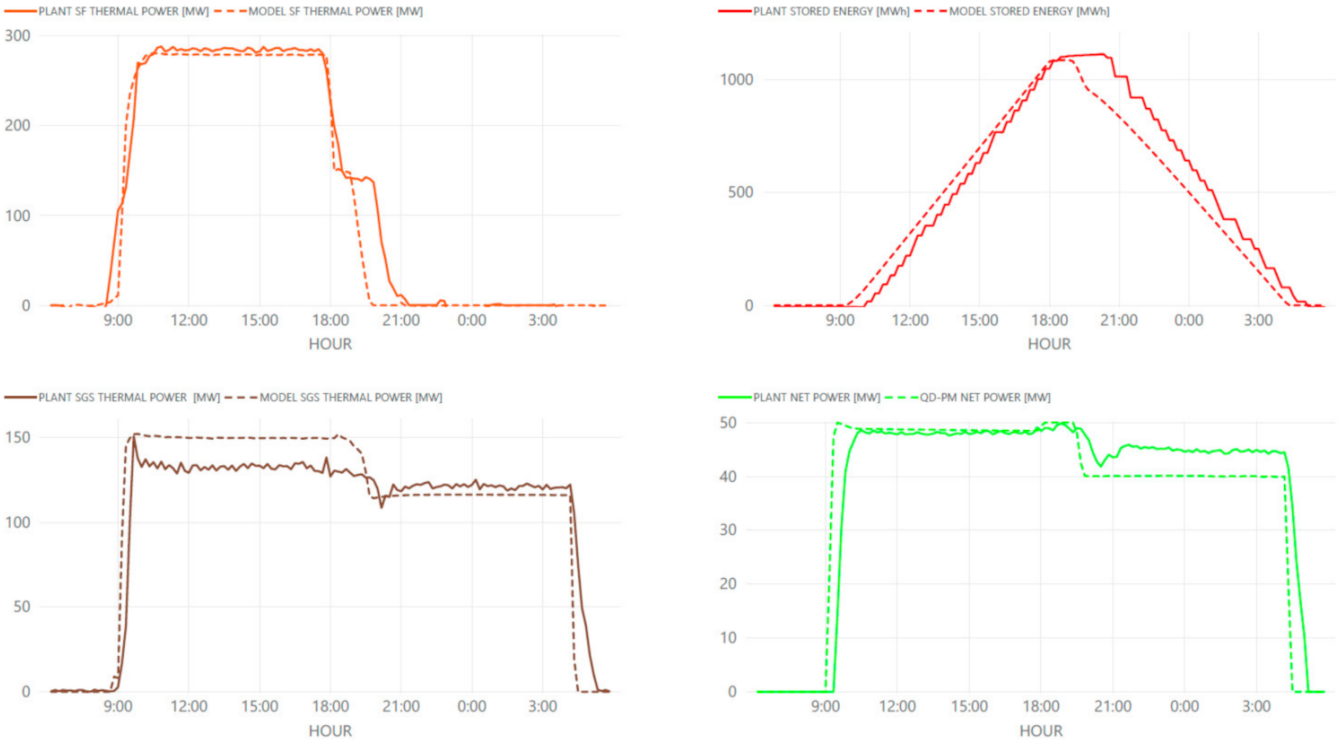

(**b**) 26th of August

Figure 14. *Cont*.

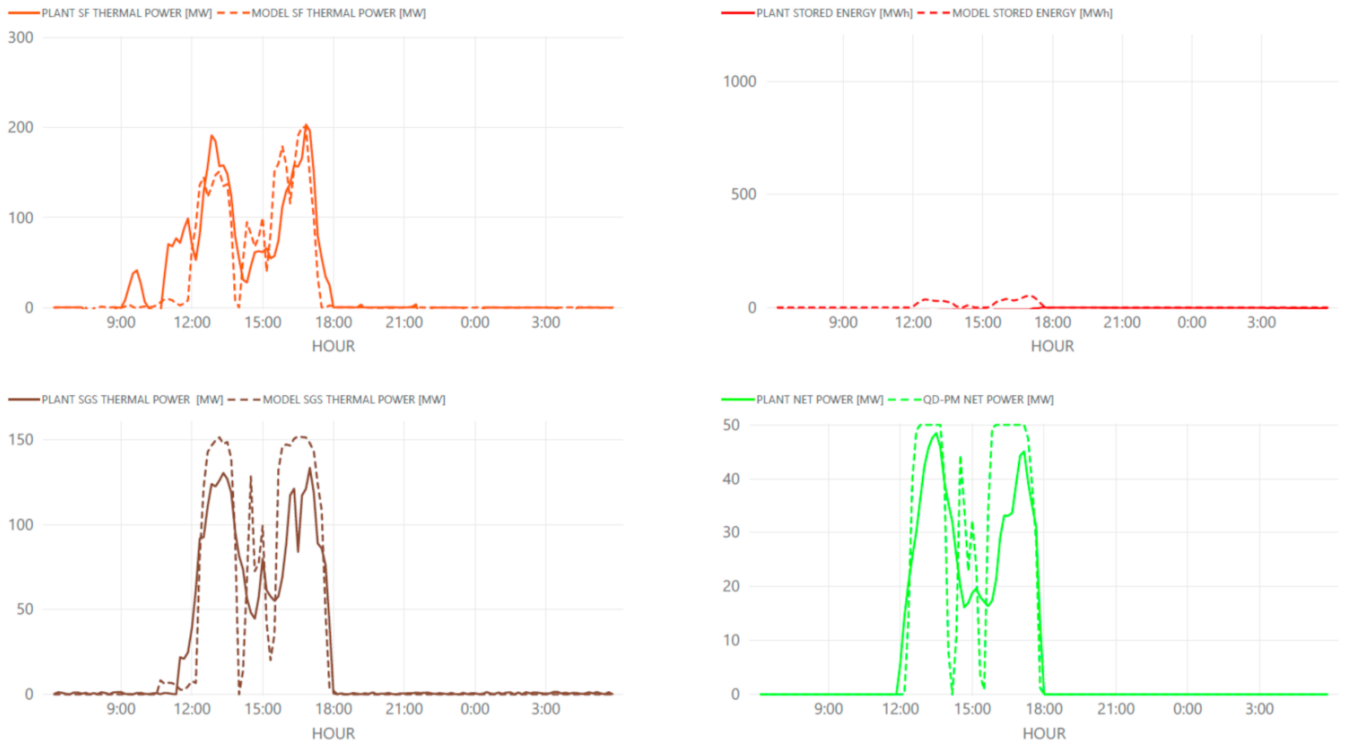

(**c**) 26th of October

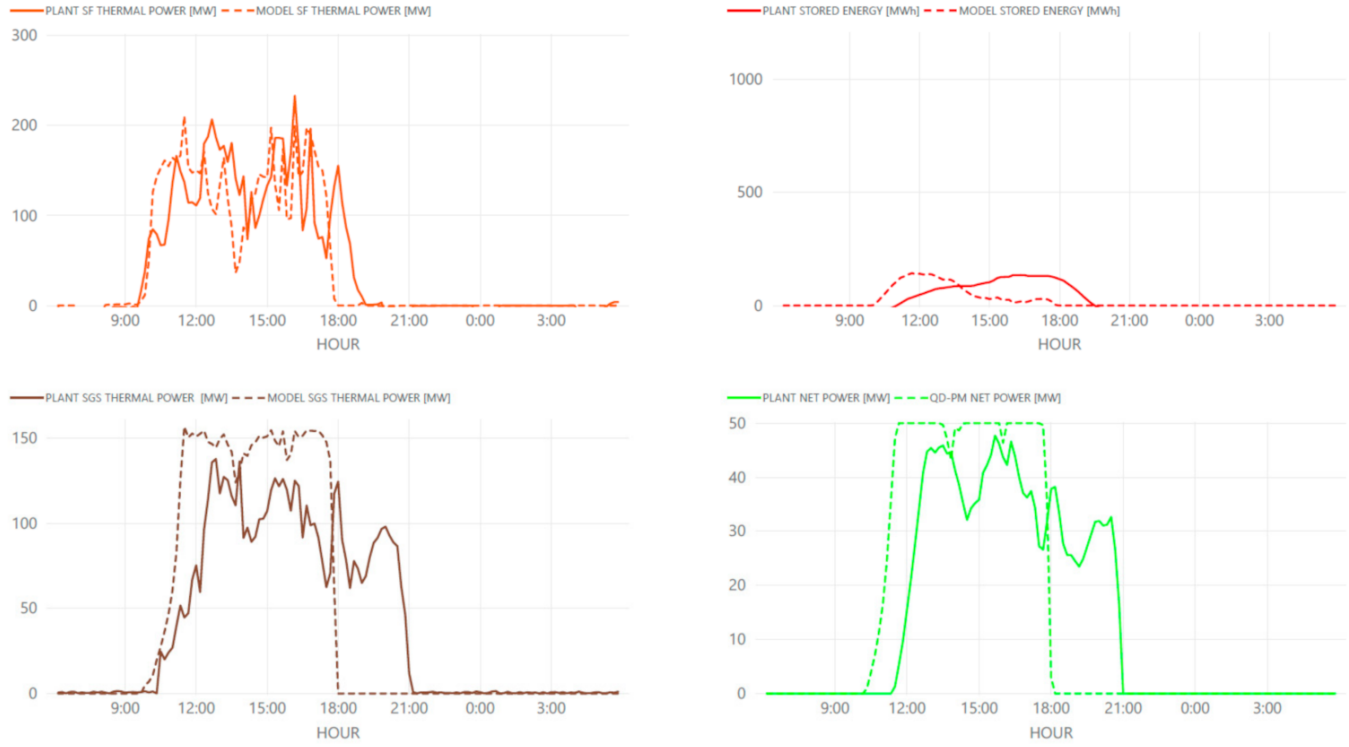

(**d**) 26th of December

Figure 14. Samples of daily comparison between QD-PM and measured data (**a**) 26th April; (**b**) 26th August; (**c**) 26th October; (**d**) 26th December.

6. Conclusions

CSP plant EPC projects can last more than five years if the proposal stage is considered. In all project stages, PM is a tool of great importance. It is mandatory to give the PM to the client as a guarantee evaluation tool when the EPC contract is signed.

In addition, when the plant is handed to the O&M team, it will also be a big help for continuously improving the operation of the plant.

CSP technology is getting new automation every year but it is still very dependent on the human factor. Operators are the ones responsible for changing the mode at all times, considering every main plant system state. These operation modes depend on both the plant and the country, the PM should be capable of emulate them all. The CSP plant performance models are mainly focused on giving an accurate value for the net energy exported to the grid because it is the data needed in the feasibility studies. Other models are focused on obtaining the best accuracy using as-build design and tracking parameters. These approaches are also very interesting, but an engineering company will ask for a PM, easy to develop and useful for all project stages. The goal of this development was to obtain a CSP plant performance model that was good enough for the feasibility stage, that can also be used in the design stage and besides, with minor changes, for performance follow up during operation.

Defining the PM with a modular approach allows the reuse of previous developments and easily add new ones. The integration wrapper simulates the transition between operation modes, including the transients between them. Some systems are very specific of CSP technology like SF and TES. But, others, like the Rankine cycle, are not specific, and otherwise, are extremely complex. A very high accuracy with satisfactory development time can be obtained by using specialized software for these systems. The static simulation of the Power Cycle is made using Thermoflex, and the dynamic performance is emulated using a meshed grid of static models. That is why the model is denominated as quasi-dynamic (QD-PM). The integration of a reliable and well-known software guarantees better results and a quicker learning curve. Furthermore, the integration of all subsystem models (SF, TES, SSG, ...) are made with a wrapper model developed using Matlab-Simulink. The parasitic electric consumption is calculated using Fathom software.

The design and implementation focused on meeting all PM requirements called for by EPC engineering. Then, the QD-PM is capable of:

- Simulating the plant's behaviour in a time step of 10 s or greater, thus studying the effect of transient operation and the effect of rapid changes in meteorological conditions.
- Modelling systems, like the Rankine cycle and all the main pumps, using a reliable specific software. This provides a much higher accuracy.
- Integrating the different subsystem models through a control algorithm based on supplier's data (related to the operation limits of materials and equipment).
- Predicting not only the net energy exported to the grid but several more variables.
- Giving a very good accuracy, as good as the one used as reference by the clients.

QD-PM outputs were validated with a complete one-year real data obtained from a 50 MW CSP plant, situated in the south of Spain, showing very good accuracy in the aggregate values and an extremely good fit regarding changes between operating modes. Results also show the differences occurred when the operator management differs from the maximum production QD-PM operating strategy. Other interesting aspect is the difference in thermal inertia, due to two factors: the dissimilarity between initial design and as-build plant, and the limitation of the quasi-dynamic approach against a complete dynamic one. Nevertheless, development time savings are preferable against the very low difference in accuracy.

Author Contributions: The model main design schema is made by R.P.M. and the final design has contribution of all authors. Methodology of research was discussed for R.P.M., J.V.A.C. and V.R.M. Implementation was mainly made by A.G.G. The tuning of the model was made by A.G.G. and J.V.A.C.

Validation are made by J.V.B., V.R.M. and A.G.G. Writing the original draft was made by J.V.A.C. and A.G.G. All the author participated in review and editing it. All authors have read and agreed to the published version of the manuscript.

Funding: This work was developed under the SOLARSIM project, funded by the Spanish government and the GRUPIN program in the University of Oviedo.

Institutional Review Board Statement: Not applicable for studies not involving humans or animals.

Informed Consent Statement: Informed consent was obtained from all subjects involved in the study.

Data Availability Statement: Restrictions apply to the availability of these data. Data was obtained from TSK and are available from the authors with the permission of TSK.

Acknowledgments: The authors would like to thank Miguel Barro, Adrián Riesgo and Sara Lopez for their support in the team effort made to understand how a CSP plant works and how can it be simulated.

Conflicts of Interest: The authors declare no conflict of interest.

Nomenclature

ACC	Air Cooled Condenser
BMU	Federal Ministry of the Environment, Nature Conservation and Nuclear Safety
BOP	Balance of Plant
CCTV	Closed-Circuit Television
CSP	Concentrated Solar Power
DCS	Distributed Control System
DNI	Direct Normal Irradiation
EPC	Engineering Procurement Construction
FH	Fuel Heaters
HCE	Heat Collector Element
HPT	High Pressure Turbine
HRSG	Heat Recovery Steam Generator
HTF	Heat Transfer Fluid
HVAC	Heating Ventilation and Air Conditioning
HX	Heat Exchangers
IAM	Incident Angle Modifier
KKS	Kraftwerk Kennzeichen System
LCOE	Levelized Cost of Energy
LD	Liquidation Damages
LPT	Low Pressure Turbine
MIMO	Multiple Inputs Multiple Outputs
NG	Natural Gas
NREL	National Renewable Energy Laboratory
O&M	Operation and Maintenance
PAC	Provisional Acceptance Certificate
PM	Performance Model
PPA	Power Purchase Agreement
PT	Parabolic Trough
PV	Photovoltaics
R&D	Research and Development
SAM	System Advisory Model
SCA	Solar Collector Assembly
SCE	Solar Collector Element
SEGS	Solar Energy Generating Systems
SF	Solar Field
SGS	Steam Generation System
SPA	Solar Position Algorithm
SSG	Solar Steam Generator
ST	Steam Turbine
TES	Thermal Energy Storage
TMY	Typical Meteorological Year
TOD	Time of Day
UTC	Coordinated Universal Time
VBA	Visual Basic for Applications
VFD	Variable Frequency Drive
WTP	Water Treatment Plant

References

1. Hirsch, T. *SolarPACES Guideline for Bankable STE Yield Assessment*; SolarPACES: Tabernas, Spain, 2017.
2. Siva Reddy, V.; Kaushik, S.C.; Ranjan, K.R.; Tyagi, S.K. State-of-the-art of solar thermal power plants—A review. *Renew. Sust. Energy Rev.* **2013**, *27*, 258–273. [CrossRef]
3. Chaanaoui, M.; Vaudreuil, S.; Bounahmidi, T. Benchmark of Concentrating Solar Power Plants: Historical, Current and Future Technical and Economic Development. *Procedia Comput. Sci.* **2016**, *83*, 782–789. [CrossRef]
4. Lilliestam, J. *Whither CSP? Taking Stock of a Decade of Concentrating Solar Power Expansion and Development*; MUSTEC: Zurich, Switzerland, 2018; p. 57.
5. Desideri, U.; Campana, P.E. Analysis and comparison between a concentrating solar and a photovoltaic power plant. *Appl. Energy* **2014**, *113*, 422–433. [CrossRef]
6. Stutz, B.; Le Pierres, N.; Kuznik, F.; Johannes, K.; Palomo Del Barrio, E.; Bédécarrats, J.-P.; Gibout, S.; Marty, P.; Zalewski, L.; Soto, J.; et al. Storage of thermal solar energy. *Comptes Rendus Phys.* **2017**, *18*, 401–414. [CrossRef]
7. Huang, W.; Hu, P.; Chen, Z. Performance simulation of a parabolic trough solar collector. *Sol. Energy* **2012**, *86*, 746–755. [CrossRef]
8. Luo, N.; Yu, G.; Hou, H.J.; Yang, Y.P. Dynamic Modeling and Simulation of Parabolic Trough Solar System. *Energy Procedia* **2015**, *69*, 1344–1348. [CrossRef]
9. Xu, L.; Wang, Z.; Li, X.; Yuan, G.; Sun, F.; Lei, D. Dynamic test model for the transient thermal performance of parabolic trough solar collectors. *Sol. Energy* **2013**, *95*, 65–78. [CrossRef]
10. Rongrong, Z.; Yongping, Y.; Qin, Y.; Yong, Z. Modeling and Characteristic Analysis of a Solar Parabolic Trough System: Thermal Oil as the Heat Transfer Fluid. *J. Renew. Energy* **2013**, *2013*, 389514. [CrossRef]
11. Barcia, L.; Peón Menéndez, R.; Martínez Esteban, J.; José Prieto, M.; Martín Ramos, J.; de Cos Juez, F.; Nevado Reviriego, A. Dynamic Modeling of the Solar Field in Parabolic Trough Solar Power Plants. *Energies* **2015**, *8*, 13361–13377. [CrossRef]
12. Abutayeh, M.; Alazzam, A. Adapting Steady-State Solar Power Models to Include Transients. *J. Sol. Energy Eng.* **2017**, *139*, 021006. [CrossRef]
13. Llorente García, I.; Álvarez, J.L.; Blanco, D. Performance model for parabolic trough solar thermal power plants with thermal storage: Comparison to operating plant data. *Sol. Energy* **2011**, *85*, 2443–2460. [CrossRef]
14. Zaversky, F.; García-Barberena, J.; Sánchez, M.; Astrain, D. Probabilistic modeling of a parabolic trough collector power plant—An uncertainty and sensitivity analysis. *Sol. Energy* **2012**, *86*, 2128–2139. [CrossRef]
15. Stoddard, M.; Faas, S.; Chiang, C.; Dirks, J. *SOLERGY: A Computer Code for Calculating the Annual Energy from Central Receiver Power Plants*; SAND86-8060; Sandia National Laboratory: Albuquerque, NM, USA, 1987.
16. Lippke, F. *Simulation of the Part-Load Behavior of a 30 MWe SEGS Plant*; SAND-95-1293; Sandia National Laboratory: Albuquerque, NM, USA, 1995.
17. Price, H.W. Validation of the FLAGSOL Parabolic Trough Solar Power Plant Performance Model. In Proceedings of the ASME/JSMEIJSES International Solar Energy Conference, Lahaina, HI, USA, 19–24 March 1995; Volume 8.
18. Price, H. A Parabolic Trough Solar Power Plant Simulation Model. In Proceedings of the ASME 2003 International Solar Energy Conference, Kohala Coast, HI, USA, 15–18 March 2003; pp. 665–673.
19. Patnode, A. Simulation and Performance Evaluation of Parabolic Trough Solar Power Plants. Master's Thesis, University of Winconsin-Madison, Madison, WI, USA, 2006.
20. Manzolini, G.; Giostri, A.; Saccilotto, C.; Silva, P.; Macchi, E. Development of an innovative code for the design of thermodynamic solar power plants part A: Code description and test case. *Renew. Energy* **2011**, *36*, 1993–2003. [CrossRef]
21. Wagner, M.; Blair, N.; Dobos, A. *A Detailed Physical Trough model for NREL's Solar Advisor Model: Preprint*; NREL/CP-5500-49368; National Renewable Energy Lab. (NREL): Golden, CO, USA, 2010; Volume 11.
22. Dobos, A.; Neises, T.; Wagner, M. Advances in CSP Simulation Technology in the System Advisor Model. *Energy Procedia* **2014**, *49*, 2482–2489. [CrossRef]
23. Guzman, L.; Henao, A.; Vasquez, R. Simulation and Optimization of a Parabolic Trough Solar Power Plant in the City of Barranquilla by Using System Advisor Model (SAM). *Energy Procedia* **2014**, *57*, 497–506. [CrossRef]
24. Ho, C.K. *Software and Codes for Analysis of Concentrating Solar Power Technologies*; SAND2008-8053; Sandia National Laboratory: Albuquerque, NM, USA, 2008.
25. Meybodi, M.A.; Ramirez Santigosa, L.; Beath, A.C. A study on the impact of time resolution in solar data on the performance modelling of CSP plants. *Renew. Energy* **2017**, *109*, 551–563. [CrossRef]
26. Larrañeta, M.; Moreno-Tejera, S.; Lillo-Bravo, I.; Silva-Pérez, M.A. Cloud transient characterization in different time steps. *AIP Conf. Proc.* **2017**, *1850*, 140016.
27. Ramorakane, R.J.; Dinter, F. Evaluation of parasitic consumption for a CSP plant. *AIP Conf. Proc.* **2016**, *1734*, 070027.
28. Reda, I.; Andreas, A. *Solar Position Algorithm for Solar Radiation Applications (Revised)*; NREL/TP-560-34302; NREL: Golden, CO, USA, 2008.
29. Burkholder, F.; Kutscher, C. *Heat Loss Testing of Schott's 2008 PTR70 Parabolic Trough Receiver*; NREL/TP-550-45633; NREL: Golden, CO, USA, 2009.
30. Shah, R.K.; Sekulić, D.P. *Fundamentals of Heat Exchanger Design*; John Wiley & Sons: Hoboken, NJ, USA, 2003; ISBN 978-0-471-32171-2.